

A Hole torn by QCD Fields.

R.S. Longacre^a

^aBrookhaven National Laboratory, Upton, NY 11973, USA

Abstract

In this paper we determine that a local negative correlation (the Hole) in $\Delta\eta$ $\Delta\phi$ space of Au + Au collisions at $\sqrt{s_{NN}}=200$ GeV is caused by strong color QCD electric and magnetic fields which are present in the Glasma Flux Tubes that are generated by the initial conditions.

1 Introduction and review of the model

In this paper we discuss a Glasma Flux Tube Model (GFTM)[1] which has tubes of parallel strong color QCD electric and magnetic fields that are generated by the initial conditions of Au + Au central collisions at $\sqrt{s_{NN}}=200$ GeV.

The paper is organized in the following manner:

Sec. 1 is the introduction and review of the model. Sec. 2 discuss two particle angular correlation in the model. Sec. 3 gives the properties of the GFTM. Sec. 4 is a comparison of charge independent two particle angular correlation between the model and the Au + Au data. Sec. 5 is a comparison of the charge dependent correlation of the signal coming from a single flux tube with the Au + Au data. Sec. 6 is about QCD and the strong CP violation term. Sec. 7 considers color electric fields and data. Sec. 8 considers color magnetic fields and data. Sec. 9 presents the summary and discussion.

1.1 Glasma Flux Tube Model

A glasma flux tube model (GFTM)[1] that had been developed considers that the wave functions of the incoming projectiles, form sheets of color glass condensates (CGC)[2] that at high energies collide, interact, and evolve into high intensity color electric and magnetic fields. This collection of primordial fields is the Glasma[3, 4], and initially it is composed of only rapidity independent longitudinal color electric and magnetic fields. An essential feature of the Glasma is that the fields are localized in the transverse space of the collision zone with a size of $1/Q_s$. Q_s is the saturation momentum of partons in the nuclear wave function. These longitudinal color electric and magnetic fields generate topological Chern-Simons charge[5] which becomes a source for particle production.

The transverse space is filled with flux tubes of large longitudinal extent but small transverse size $\sim Q_s^{-1}$. Particle production from a flux tube is a Poisson process, since the flux tube is a coherent state. The flux tubes at the center of the transverse plane interact with each other through plasma instabilities[3, 6] and create a locally thermalized system, where

partons emitted from these flux tubes are locally equilibrated. A hydro system with transverse flow builds causing a radially flowing blast wave[7]. The flux tubes that are near the surface of the fireball get the largest radial flow and are emitted from the surface.

Q_s is around 1 GeV/c thus the transverse size of the flux tube is about 1/4 fm. The flux tubes near the surface are initially at a radius ~ 5 fm. The ϕ angle wedge of the flux tube is $\sim 1/20$ radians or $\sim 3^\circ$. Thus the flux tube initially has a narrow range in ϕ . The width in $\Delta\eta$ correlation of particles results from the independent longitudinal color electric and magnetic fields that created the Glasma flux tubes. In this paper we relate particle production from the surface flux tube to a related model Parton Bubble Model(PBM)[8]. It was shown in Ref.[9] that for central Au + Au collisions at $\sqrt{s_{NN}}=200$ the PBM is a good approximation to the GFTM surface flux tube formation.

The flux tubes on the surface turn out to be on the average 12 in number. They form an approximate ring about the center of the collision see Figure 1. The twelve tube ring creates the average behavior of tube survival near the surface of the expanding fire ball of the blast wave. The final state surface tubes that emit the final state particles at kinetic freezeout are given by the PBM. One should note that the blast wave surface is moving at its maximum velocity at freezeout ($3c/4$).

The space momentum correlation of the blast wave provides us with a strong angular correlation signal. PYTHIA fragmentation functions[10] were used for the tube fragmentation that generate the final state particles emitted from the tube. The initial transverse size of a flux tube $\sim 1/4$ fm has expanded to the size of ~ 2 fm at kinetic freezeout. Many particles that come from the surface of the fireball will have a p_t greater than 0.8 GeV/c. The final state tube size and the Hanbury-Brown and Twiss (HBT) observations[11] of pions that have a momentum range greater than 0.8 GeV/c are consistent both being ~ 2 fm. A single parton using PYTHIA forms a jet with the parton having a fixed η and ϕ (see Figure 2). For central events each of the twelve tubes have 3-4 partons per tube each at a fixed ϕ for a given tube. The p_t distribution of the partons is similar to pQCD but has a suppression at high p_t like the data. The 3-4 partons in the tube which shower using PYTHIA all have a different η values but all have the same ϕ (see Figure 3). The PBM explained the high precision Au + Au central (0-10%) collisions at $\sqrt{s_{NN}} = 200$ GeV[12](the highest RHIC energy).

2 The Correlation Function for Central Au + Au Data

We utilize a two particle correlation function in the two dimensional (2-D) space¹ of $\Delta\phi$ versus $\Delta\eta$. The 2-D total correlation function is defined as:

$$C(\Delta\phi, \Delta\eta) = S(\Delta\phi, \Delta\eta)/M(\Delta\phi, \Delta\eta). \quad (1)$$

¹ $\Delta\phi = \phi_1 - \phi_2$ where ϕ is the azimuthal angle of a particle measured in a clockwise direction about the beam. $\Delta\eta = \eta_1 - \eta_2$ which is the difference of the pseudorapidity of the pair of particles

Plane section of tube geometry perpendicular to the beam at $\eta = 0$

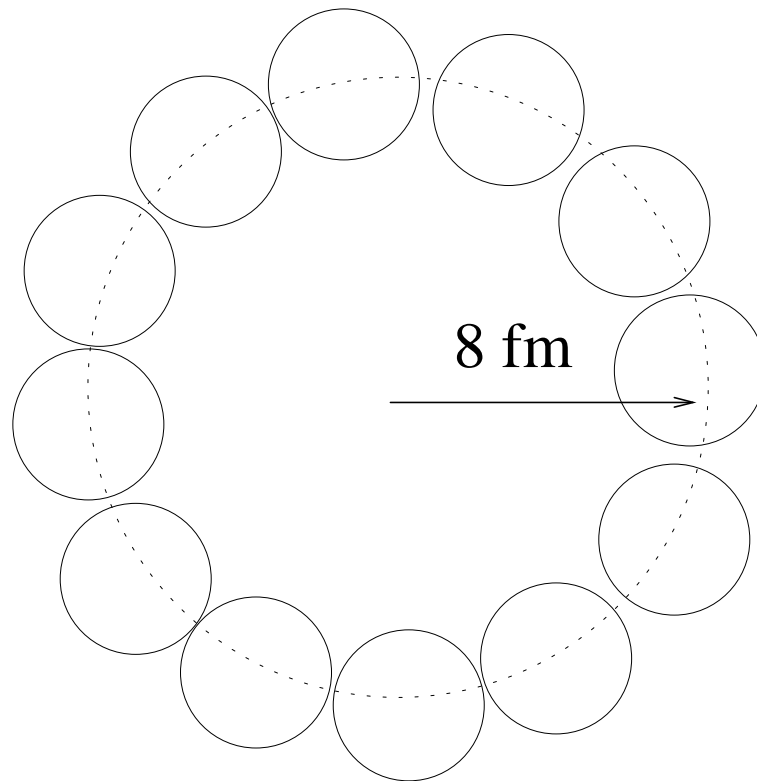


Figure 1: The tube geometry is an 8 fm radius ring perpendicular to and centered on the beam axis. It is composed of twelve adjacent 2 fm radius circular tubes elongated along the beam direction as part of the flux tube geometry. We project on a plane section perpendicular to the beam axis.

Jet

Parton Shower

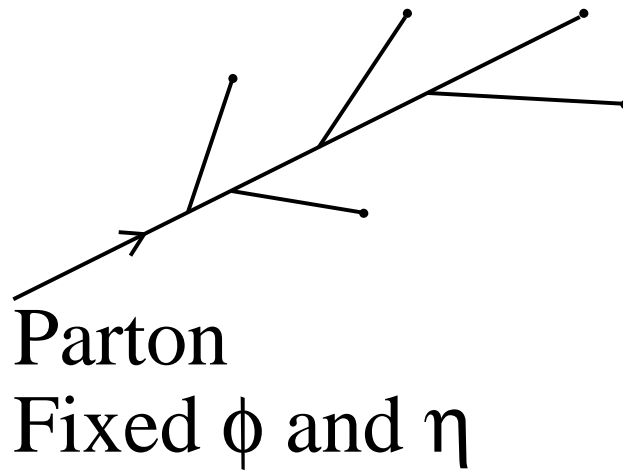
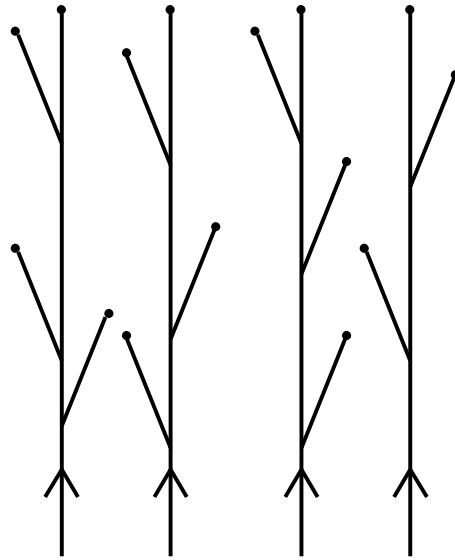


Figure 2: A jet parton shower.

Partons in a Tube



3-4 Partons
Fixed ϕ Different η

Figure 3: Each tube contains 3-4 partons as shown.

Where $S(\Delta\phi, \Delta\eta)$ is the number of pairs at the corresponding values of $\Delta\phi, \Delta\eta$ coming from the same event, after we have summed over all the events. $M(\Delta\phi, \Delta\eta)$ is the number of pairs at the corresponding values of $\Delta\phi, \Delta\eta$ coming from the mixed events, after we have summed over all our created mixed events. A mixed event pair has each of the two particles chosen from a different event. We make on the order of ten times the number of mixed events as real events. We rescale the number of pairs in the mixed events to be equal to the number of pairs in the real events. This procedure implies a binning in order to deal with finite statistics. The division by $M(\Delta\phi, \Delta\eta)$ for experimental data essentially removes or drastically reduces acceptance and instrumental effects. If the mixed pair distribution was the same as the real pair distribution $C(\Delta\phi, \Delta\eta)$ should have unit value for all of the binned $\Delta\phi, \Delta\eta$. In the correlations used first in this paper we select particles independent of its charge. The correlation of this type is called a Charge Independent (CI) Correlation. This difference correlation function has the defined property that it only depends on the differences of the azimuthal angle ($\Delta\phi$) and the beam angle ($\Delta\eta$) for the two particle pair. Thus the two dimensional difference correlation distribution for each tube which is part of $C(\Delta\phi, \Delta\eta)$ is similar for each of the objects and will image on top of each other. We further divide the data (see Table I) into p_t ranges (bins).

Table I. The p_t bins and the number of charged particles per bin with $|\eta| < 1.0$.

Table I	
p_t range	amount
$4.0\text{GeV}/c - 1.1\text{GeV}/c$	149
$1.1\text{GeV}/c - 0.8\text{GeV}/c$	171
$0.8\text{GeV}/c - 0.65\text{GeV}/c$	152
$0.65\text{GeV}/c - 0.5\text{GeV}/c$	230
$0.5\text{GeV}/c - 0.4\text{GeV}/c$	208
$0.4\text{GeV}/c - 0.3\text{GeV}/c$	260
$0.3\text{GeV}/c - 0.2\text{GeV}/c$	291

Since we are choosing particle pairs, we choose for the first particle p_{t1} which could be in one bin and for the second particle p_{t2} which could be in another bin. Therefore binning implies a matrix of p_{t1} vs p_{t2} . We have 7 bins thus there are 28 independent combination. Each combination will have a different number of enters. In order to take out this difference one uses multiplicity scaling[13, 14]. The diagonal bins one scales event average of Table I. For the off diagonal combination one uses the product of square root of corresponding diagonal event averages. In Figure 4 we show the correlation function equation 1 for the highest diagonal bin p_t 4.0 to 1.1 GeV/c. Figure 5 is the smallest diagonal bin p_t 0.3 to 0.2 GeV/c.

Once we use multiplicity scaling we can compare all 28 combination. In Figure 9 we show all 28 plots, but the z-axis has been rescaled so that each appear the same size. In Figure 10 we again show the 28 plots all having the same scale. This make it easier to see how fast the correlation signals drop off with lowering the momentum. These plots show the properties of parton fragmentation. P1P7 has the same signal as P2P6, P3P5, and P4P4.

P7P7

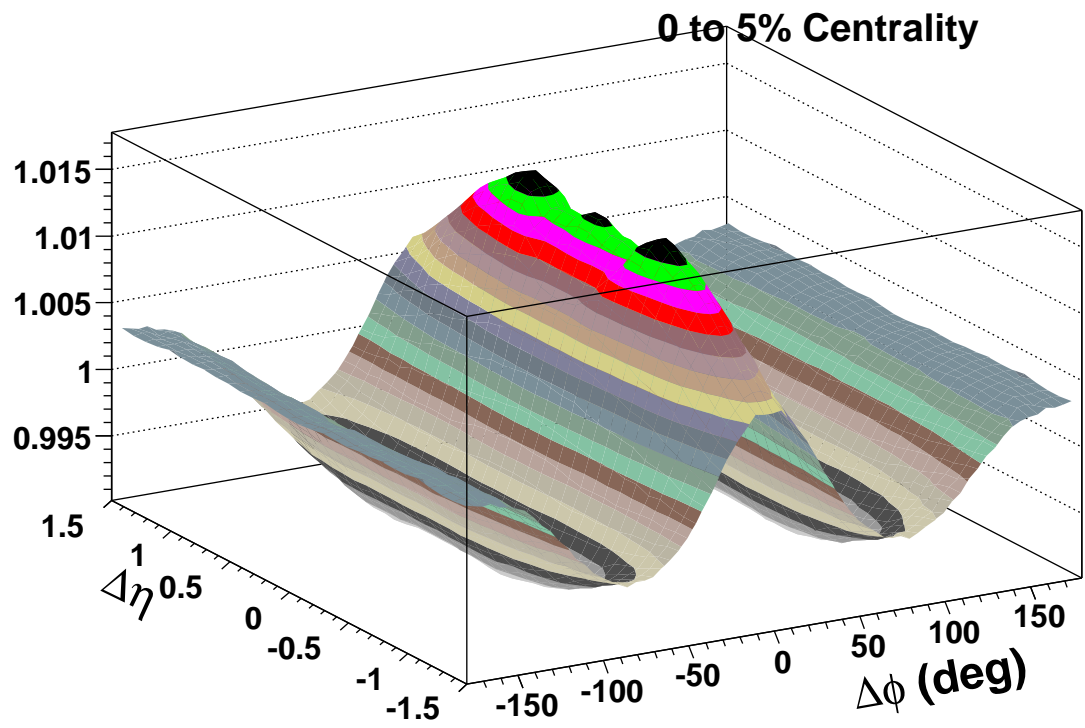


Figure 4: $\Delta\phi$ vs. $\Delta\eta$ CI correlation for the 0-5% centrality bin for Au + Au collisions at $\sqrt{s_{NN}} = 200$ GeV requiring both particles to be in bin 7 p_t greater than 1.1 GeV/c and p_t less than 4.0 GeV/c.

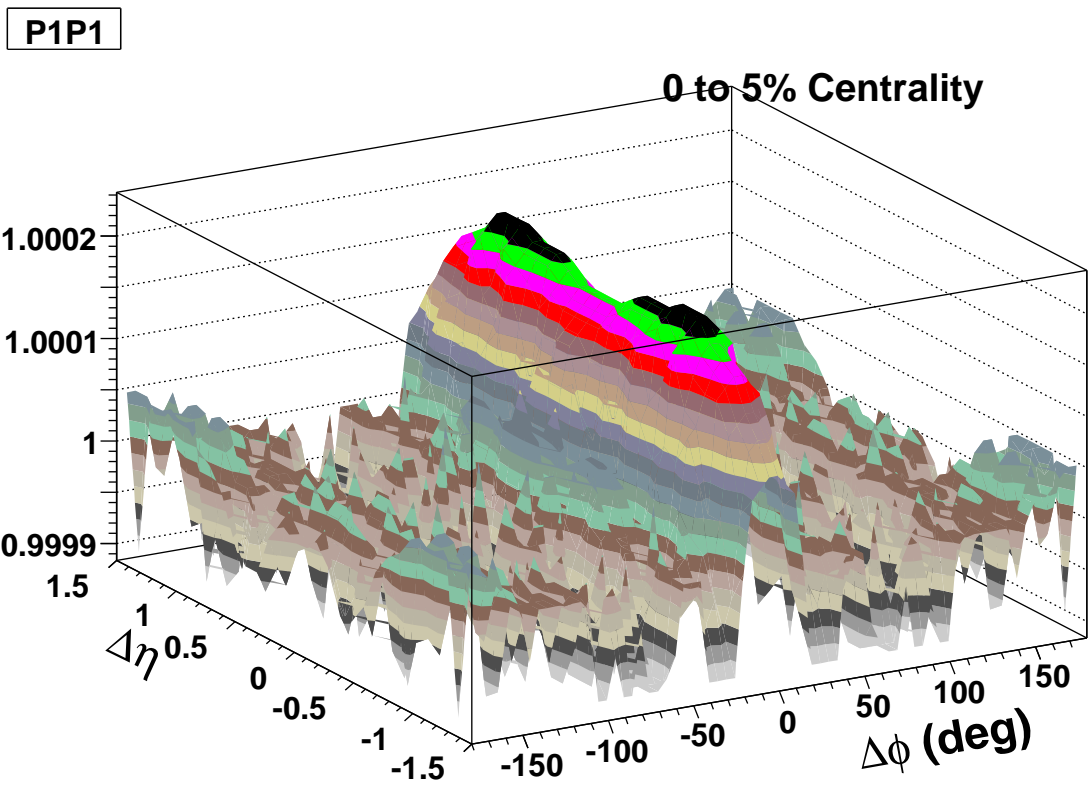


Figure 5: $\Delta\phi$ vs. $\Delta\eta$ CI correlation for the 0-5% centrality bin for Au + Au collisions at $\sqrt{s_{NN}} = 200$ GeV requiring both particles to be in bin 1 p_t greater than 0.2 GeV/c and p_t less than 0.3 GeV/c.

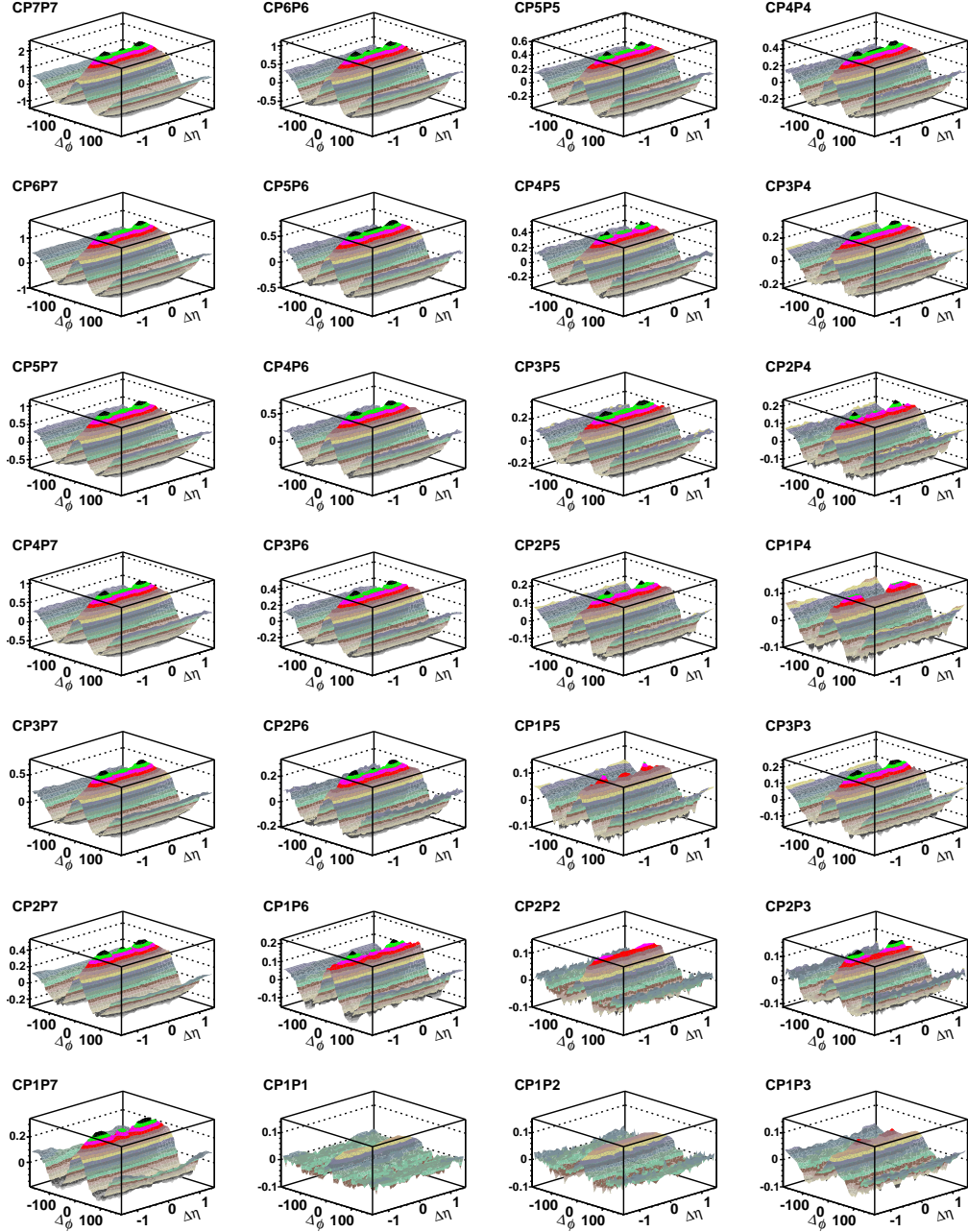


Figure 6: $\Delta\phi$ vs. $\Delta\eta$ CI correlation for the 0-5% centrality bin for Au + Au collisions at $\sqrt{s_{NN}} = 200$ GeV for all 28 combination of p_{t1} vs p_{t2} (see text).

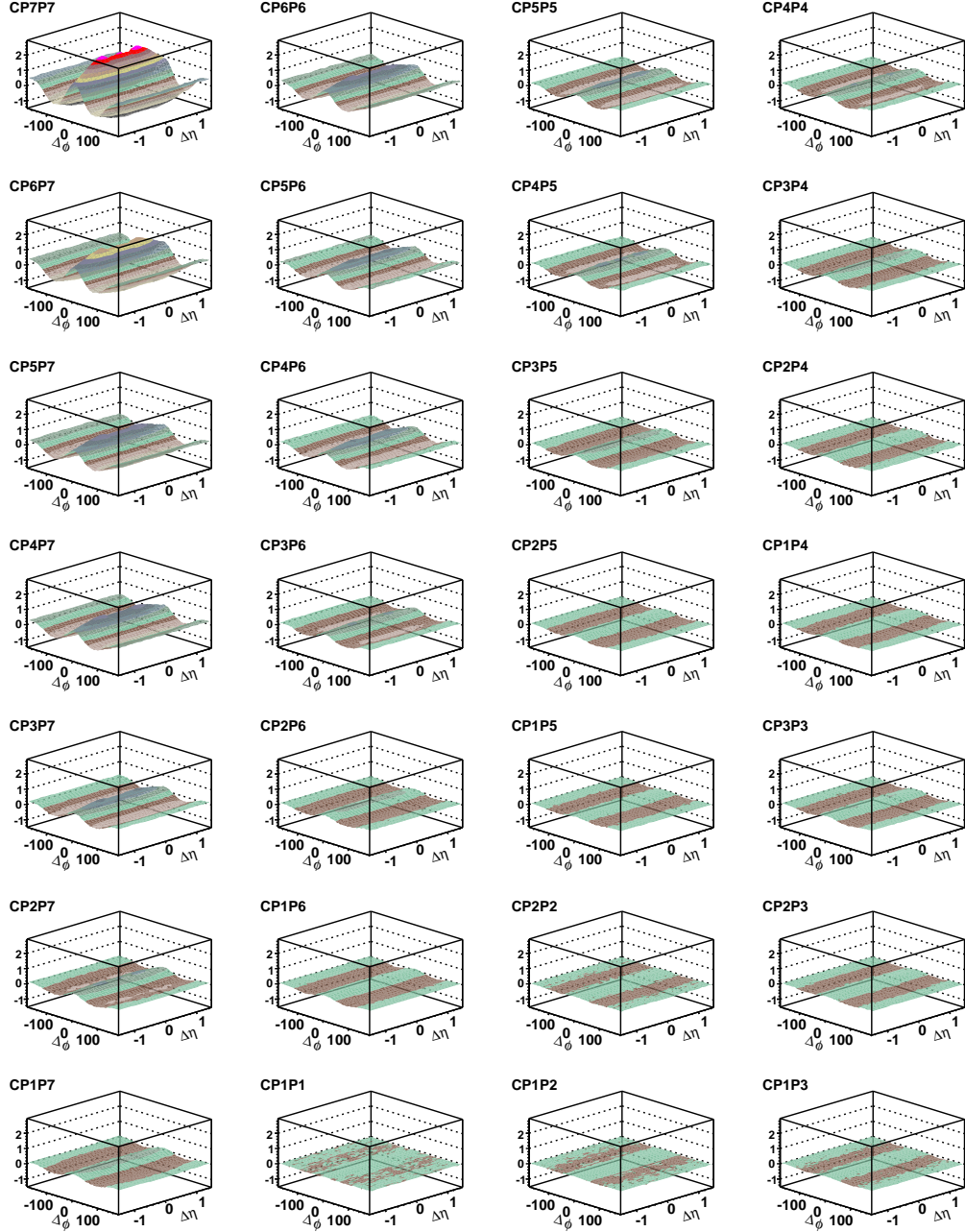


Figure 7: $\Delta\phi$ vs. $\Delta\eta$ CI correlation for the 0-5% centrality bin for Au + Au collisions at $\sqrt{s_{NN}} = 200$ GeV for all 28 combination of p_{t1} vs p_{t2} not rescaled (see text).

3 The properties of the Glasma Flux Tube Model

For the above correlations on average there was 12 final state tubes on the surface of the fireball per central Au + Au collision. Each tube on the average showered into 49 charged particles. The soft uncorrelated particles accounted for 873 or 60% of the charged particles. Since the tubes are sitting on the surface of the fireball and being push outward by radial flow, not all particles emitted from the tube will escape. Approximately one half of the particles that are on the outward surface leave the fireball and the other half are absorbed by the fireball (see Figure 8). This means that 20% of the charged particles come from tube emission, and 294 particles are added to the soft particles increasing the number to 1167 (see Table III).

Table III. Parameters of the GFTM for charged particles.

Table III		
variable	amount	fluctuations
<i>tubes</i>	12	0
<i>particles</i>	24.5	5
<i>soft</i>	1167	34

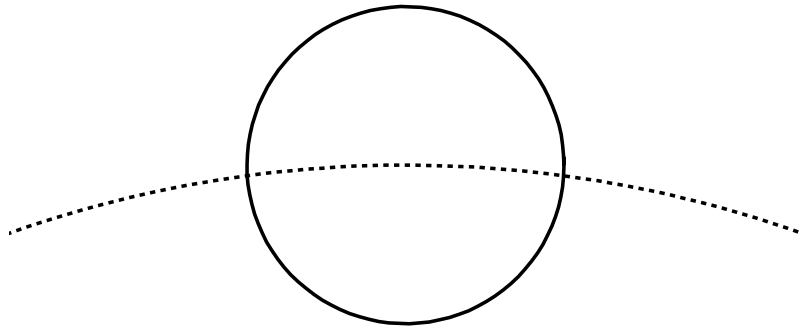
The particles that emitted outward are boosted in momentum, while the inward particles are absorbed by the fireball. Out of the initial 49 particles per tube the lower p_t particles have larger losses. In Table IV we give a detailed account of these percentage losses and give the average number of charged particles coming from each tube for each p_t bin.

Table IV. Parameters of the GFTM for p_t of the charged particles .

Table IV		
p_t	amount	%survive
$4.0\text{GeV}/c - 1.1\text{GeV}/c$	4.2	100
$1.1\text{GeV}/c - 0.8\text{GeV}/c$	3.8	76
$0.8\text{GeV}/c - 0.65\text{GeV}/c$	3.2	65
$0.65\text{GeV}/c - 0.5\text{GeV}/c$	4.2	54
$0.5\text{GeV}/c - 0.4\text{GeV}/c$	3.2	43
$0.4\text{GeV}/c - 0.3\text{GeV}/c$	3.3	35
$0.3\text{GeV}/c - 0.2\text{GeV}/c$	2.6	25

In the surface GFTM we have thermalization and hydro flow for the soft particles, while all the two particle angular correlations come from the tubes on the surface. The charge particle spectrum of the GFTM is given by a blast wave model and the direct tube fragmentation is only 20% of this spectrum. The initial anisotropic azimuthal distribution of flux tubes is transported to the final state leaving its pattern on the ring of final state flux tubes on the surface. This final state anisotropic flow pattern can be decomposed in a Fourier series (v_1, v_2, v_3, \dots). These coefficients have been measure[15] and have been found to be important in central Au + Au collisions.

In the rest frame of the tube $1/2$
of the particles are emitted away
from the fireball surface



average of 49 particles 24.5 go outward

Figure 8: Each tube sits on the surface.

4 Charge Independent Correlation compared with the Au + Au Data

How well does the glasma flux tube model (GFTM)[1][8] reproduce the Au + Au central collision data at $\sqrt{s_{NN}} = 200$ GeV. A complete analysis for Au + Au central data 0-10% within a p_t range of $0.8 < p_t < 2.0$ GeV/c can be found in Ref.[12]. Here we compare two of our p_t ranges in a $\Delta\eta$ range $0.6 < \Delta\eta < 0.9$ for Au + Au central collision data 0-5% at $\sqrt{s_{NN}} = 200$ GeV. The first p_t range bin is P7P7 where P7 is $1.1 < p_t < 4.0$ GeV/c(see Figure 9). The surface flux tube correlations are very strong in this bin. When we let one of the particles move down in p_t to P4 $0.5 < p_t < 0.65$ GeV/c(see Figure 10) the correlation weakens a lot. We see that the GFTM does a good job reproducing the charge independent data.

5 Charge dependent correlations of the signal coming from a single flux tube

In this section we are going to explore the detailed shape of the correlations coming from a single flux tube. We will follow the method used in Refs.[8, 12, 13, 14]. We can display the correlations coming from a single flux tube if we form S of equation 1, where $S(\Delta\phi, \Delta\eta)$ is the number of pairs at the corresponding values of $\Delta\phi, \Delta\eta$ coming from the same flux tube in each event. We then sum S over all the events. $M(\Delta\phi, \Delta\eta)$ remains the number of pairs at the corresponding values of $\Delta\phi, \Delta\eta$ coming from the mixed events, after we have summed over all our created mixed events. Another way to form is same correlation is to form S of equation 1 coming from all pairs except those from the same flux tube in each event(we call this the background). We then subtract this S(background) from S made out of all the pairs. If we want to display the single flux tube correlation of the data, we subtract S(background) from the S generated by the data.

In order to explore the charge dependence, we separate pairs into like sign pairs and unlike sign pairs. We will show how well GFTM describes surface flux tubes by looking at P7P7 charge dependent correlation. In Figure 11 we show the unlike sign pair correlation of the single flux tube and the background subtracted data. In Figure 12 we show the same for like sign pairs. It should be noted that when we compare the data there are some pair wise track cuts. For Figure 11 unlike sign pairs with a $\Delta\eta < 0.1$ there is a $\Delta\phi < 20^\circ$ cut and $0.1 < \Delta\eta < 0.2$ there is a $\Delta\phi < 10^\circ$ cut. These cuts remove track merging and the Coulomb effect. For Figure 12 like sign pairs with a $\Delta\eta < 0.2$ there is a $\Delta\phi < 5^\circ$ cut. These cuts remove track merging and the HBT effect.

We see in both Figure 11 and Figure 12, that the correlation from each pair choice is well described by GFTM. We see at small $\Delta\phi, \Delta\eta$ there is a local bump for unlike sign pairs, while there is negative bump or dip for like sign pairs. This dip or hole torn is caused by QCD field shown in Figure 13. This field focus unlike charge pairs into the same $\Delta\phi, \Delta\eta$ and defocus like charge pairs out of this same region.

P7P7 CI fit, $0.6 < \Delta\eta < 0.9$

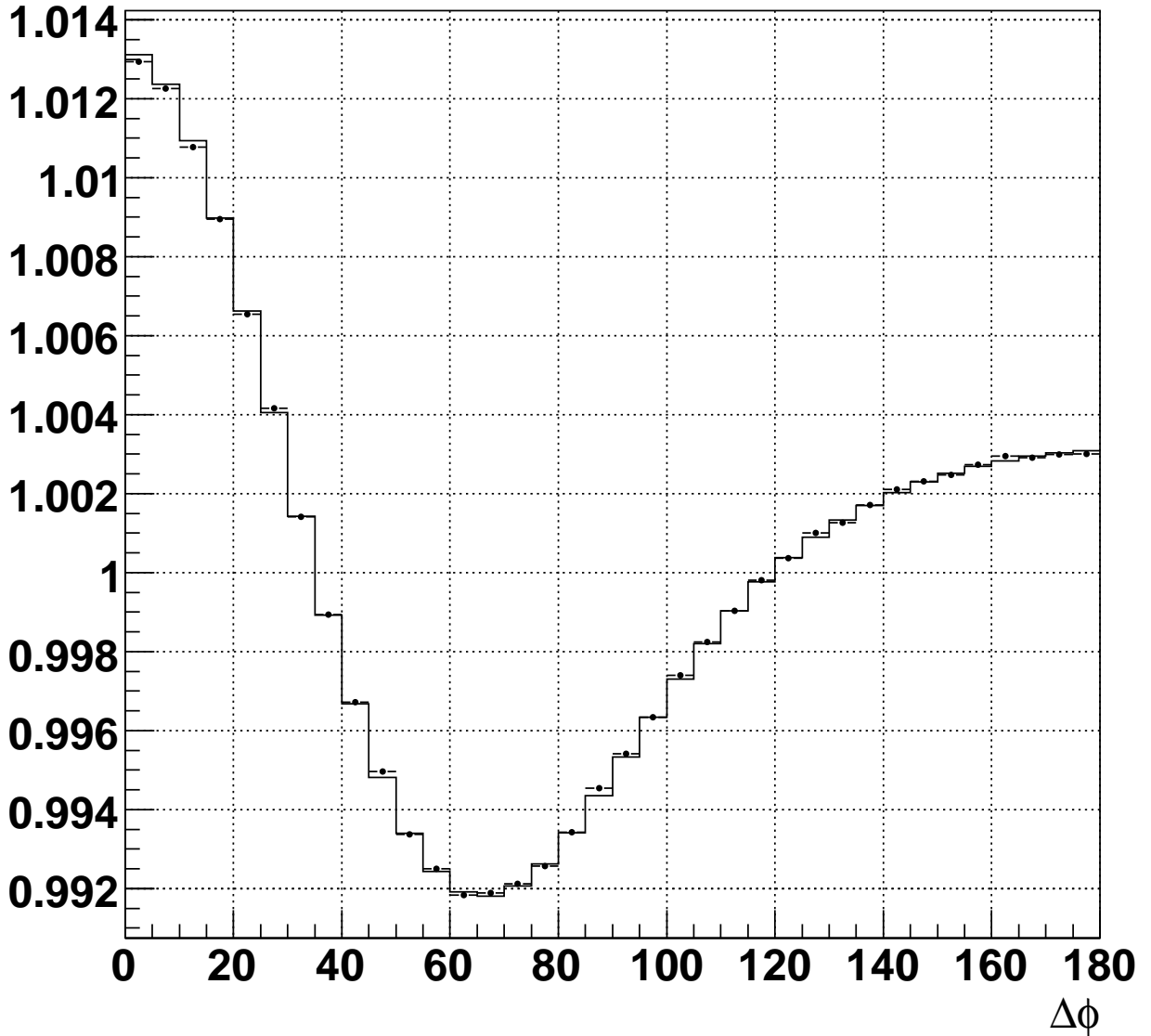


Figure 9: $\Delta\phi$ for GFTM vs Au + Au data for $\Delta\eta$ range $0.6 < \Delta\eta < 0.9$ Au + Au central collision data 0-5% at $\sqrt{s_{NN}} = 200$ GeV requiring both particles to be in bin 7 p_t greater than 1.1 GeV/c and p_t less than 4.0 GeV/c.

P4P7 CI fit, $0.6 < \Delta\eta < 0.9$

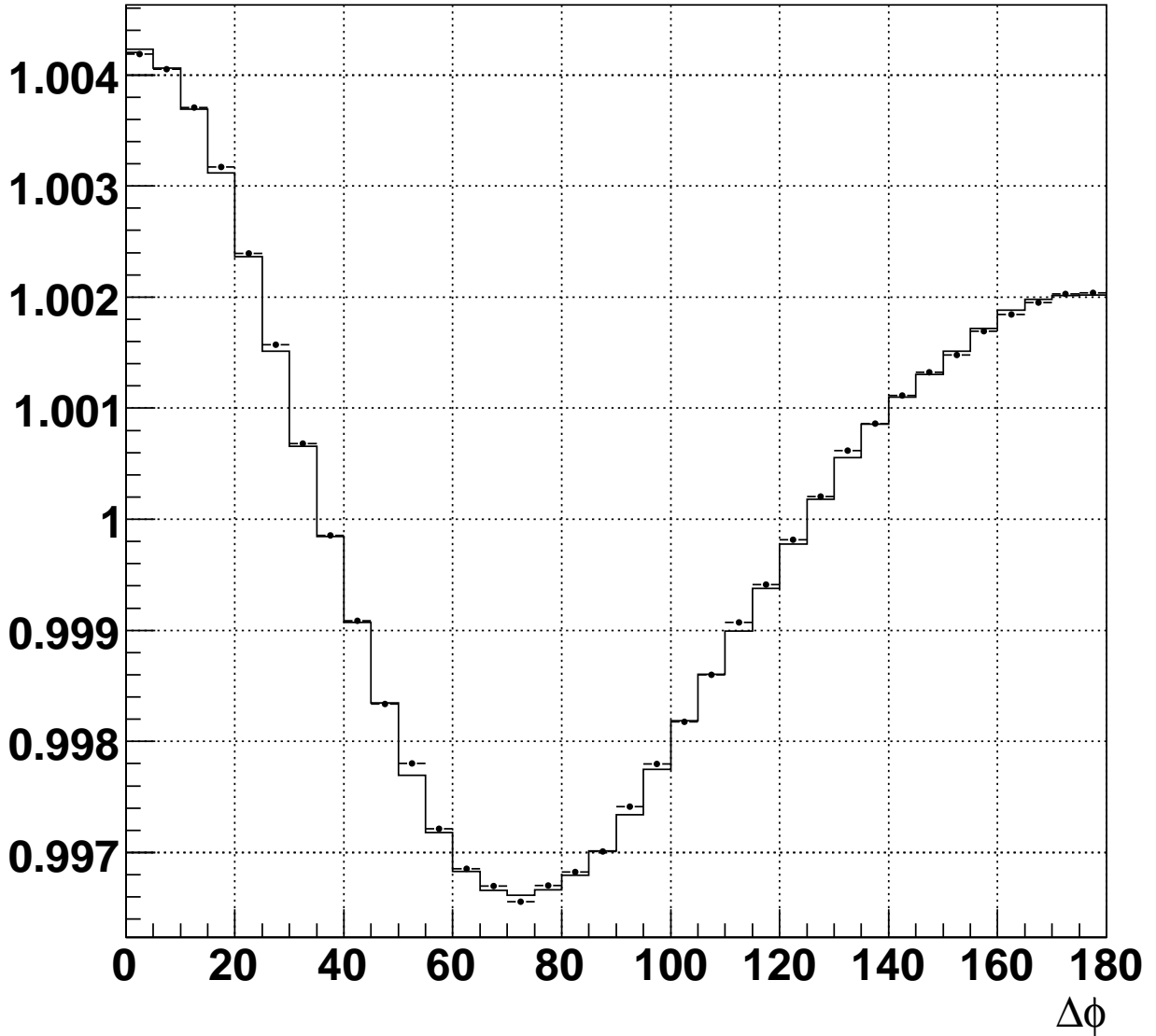
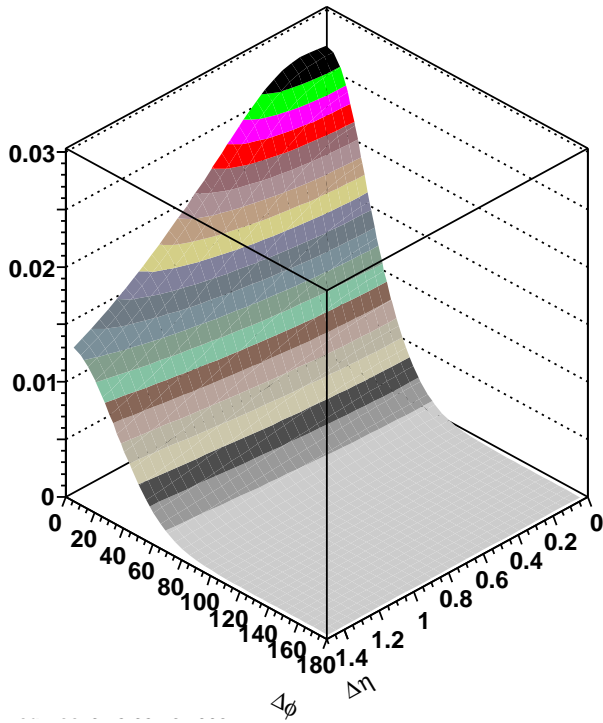


Figure 10: $\Delta\phi$ for GFTM vs Au + Au data for $\Delta\eta$ range $0.6 < \Delta\eta < 0.9$ Au + Au central collision data 0-5% at $\sqrt{s_{NN}} = 200$ GeV requiring one particle to be in bin 7 p_t greater than 1.1 GeV/c and p_t less than 4.0 GeV/c and the second to be in bin 4 p_t greater than 0.65 GeV/c and p_t less than 0.8 GeV/c.

Unlike sign signal - Run4 - centrality 0 to 5%



Unlike sign data minus background fit

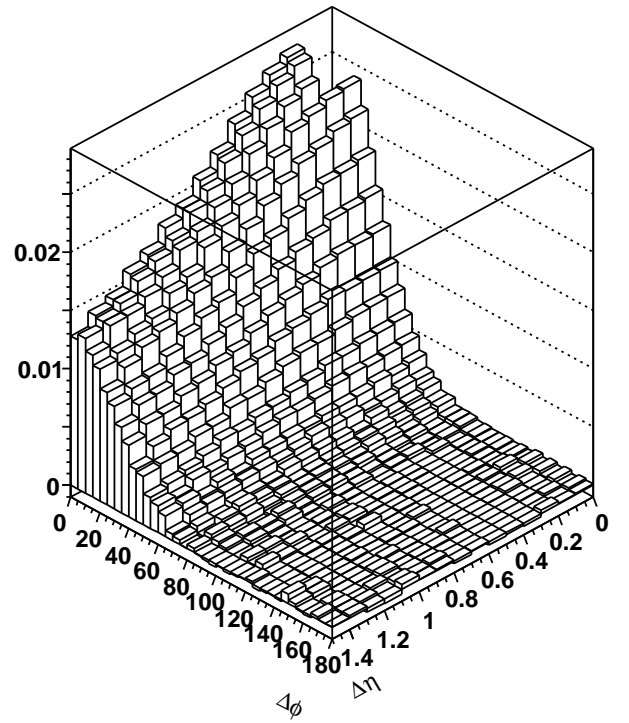
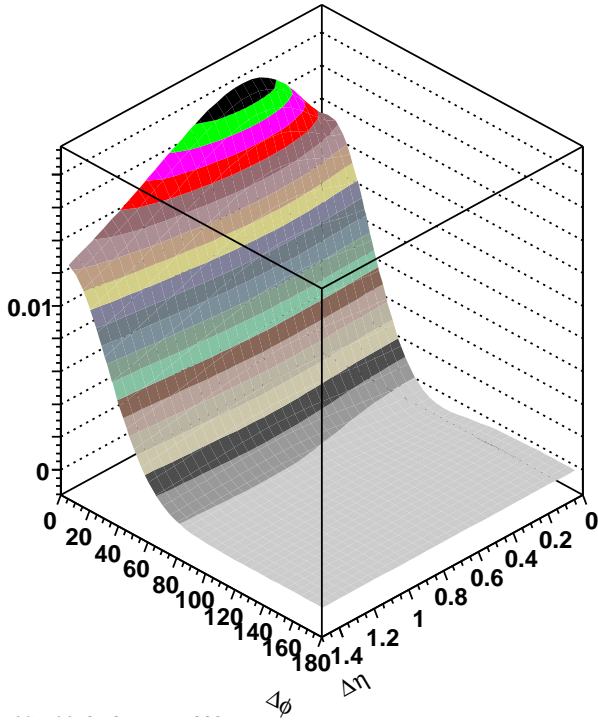


Figure 11: a) 2-D perspective plot of the unlike sign pairs for a single tube GFTM signal in Au + Au central collision data 0-5% at $\sqrt{s_{NN}} = 200$ GeV requiring both particles to be in bin 7 p_t greater than 1.1 GeV/c and p_t less than 4.0 GeV/c. b) 2-D perspective plot of the unlike sign pairs single tube data signal (see text) in Au + Au central collision data 0-5% at $\sqrt{s_{NN}} = 200$ GeV requiring both particles to be in bin 7 p_t greater than 1.1 GeV/c and p_t less than 4.0 GeV/c.

Like sign signal - Run4 - centrality 0 to 5%



Like sign data minus background fit

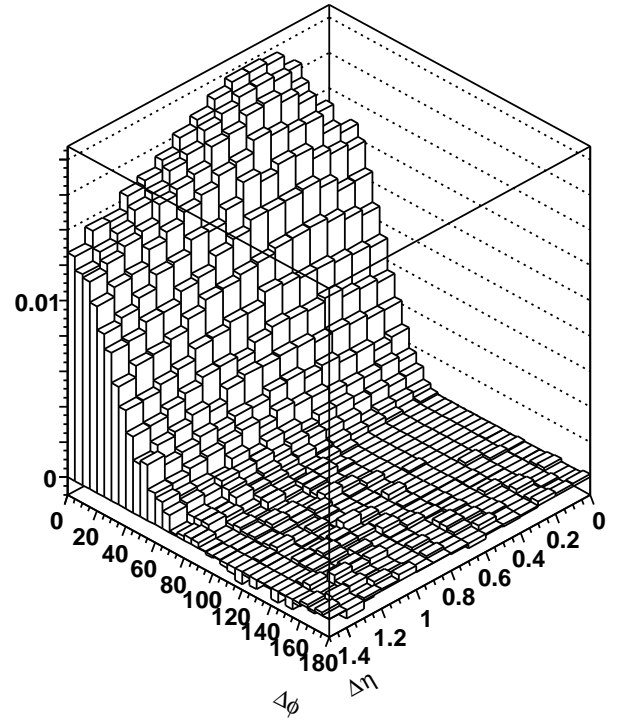


Figure 12: a) 2-D perspective plot of the like sign pairs for a single tube GFTM signal in Au + Au central collision data 0-5% at $\sqrt{s_{NN}} = 200$ GeV requiring both particles to be in bin 7 p_t greater than 1.1 GeV/c and p_t less than 4.0 GeV/c. b) 2-D perspective plot of the like sign pairs single tube data signal (see text) in Au + Au central collision data 0-5% at $\sqrt{s_{NN}} = 200$ GeV requiring both particles to be in bin 7 p_t greater than 1.1 GeV/c and p_t less than 4.0 GeV/c.

quark anti-quark pairs in a color electric field

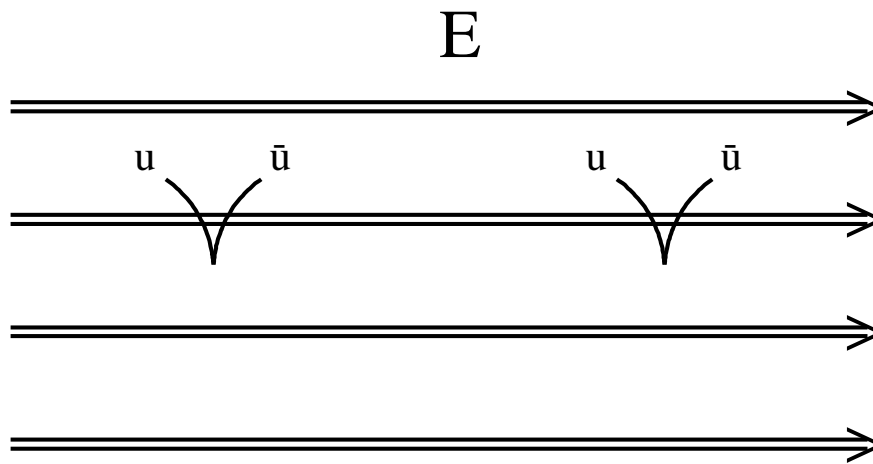


Figure 13: Inside each flux tube a large color electric field causes pairs of color and anti-color up quarks to be aligned in this field. The up quark ends up in a π^+ and the anti-up quark ends up in a π^- .

6 Strong CP violations or Chern-Simons topological charge

6.1 The Source $F\tilde{F}$.

The strong CP problem remains one of the most outstanding puzzles of the Standard Model. Even though several possible solutions have been put forward it is not clear why CP invariance is respected by the strong interaction. It was shown however through a theorem by Vafa-Witten[16] that the true ground state of QCD cannot break CP.

The part of the QCD Lagrangian that breaks CP is related to the gluon-gluon interaction term $F\tilde{F}$. The part of $F\tilde{F}$ related to CP violations can be separated into a separate term which then can be varied by multiplying this term by a parameter called θ . For the true QCD ground state $\theta = 0$ (Vafa-Witten theorem). In the vicinity of the deconfined QCD vacuum metastable domains[17] with θ non-zero could exist and not contradict the Vafa-Witten theorem since it is not the QCD ground state. The metastable domains CP phenomenon would manifest itself in specific correlations of pion momenta[17, 18].

6.2 Pionic measures of CP violation.

The glasma flux tube model (GFTM)[1] considers the wave functions of the incoming projectiles, form sheets of CGC[2] at high energies that collide, interact, and evolve into high intensity color electric and magnetic fields. This collection of primordial fields is the Glasma[3, 4]. Initially the Glasma is composed of only rapidity independent longitudinal (along the beam axis) color electric and magnetic fields. These longitudinal color electric and magnetic fields generate topological Chern-Simons charge[5] through the $F\tilde{F}$ term and becomes a source of CP violation. How much of these longitudinal color electric and magnetic fields are still present in the surface flux tubes when they have been pushed by the blast wave is a speculation of this paper for measuring strong CP violation? The color electric field which points along the flux tube axis causes an up quark to be accelerated in one direction along the beam axis, while the anti-up quark is accelerated in the other direction. So when a pair of quarks and anti-quarks are formed they separate along the beam axis leading to a separated $\pi^+ \pi^-$ pair along this axis(see Figure 13). The color magnetic field which also points along the flux tube axis (which is parallel to the beam axis) causes an up quark to rotate around the flux tube axis in one direction, while the anti-up quark is rotated in the other direction. So when a pair of quarks and anti-quarks are formed they will pick up or lose transverse momentum(see Figure 14). These changes in p_t will be transmitted to the $\pi^+ \pi^-$ pairs.

To represent the color electric field effect we assume as the first step for the results being shown in this paper; that we generate tubes which have an added boost of 100 MeV/c to the quarks in the longitudinal momentum which represents the color electric effect. The π^+ and the π^- which form a pair are boosted in opposite directions along the beam axis. In a given tube all the boosts are the same but vary in direction from tube to tube. For the color magnetic field effect, we give 100 MeV/c boosts to the transverse momentum in an opposite

quark anti-quark pairs in a color magnetic field

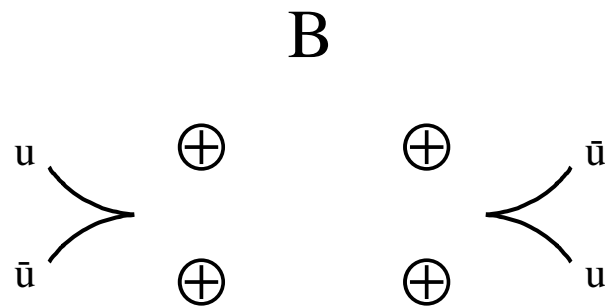


Figure 14: Inside each flux tube a large color magnetic field causes pairs of color and anti-color up quarks to be pushed away from this field causing a difference in P_t between quark and anti quark. The up quark ends up in a π^+ and the anti-up quark ends up in a π^- .

way to the π^+ and the π^- which form a pair. For each pair on one side of a tube one of the charged pions boost is increased and the other is decreased. While on the other side of the tube the pion for which the boost was increased is now decreased and the pion which was decreased is now increased by the 100 MeV/c. All pairs for a given tube are treated in the same way however each tube is random on the sign of the pion which is chosen to be boosted on a given side. This addition to our model is used in the simulations of the following sections.

7 Color electric field pionic measure and data.

Above we saw that pairs of positive and negative pions should show a charge separation along the beam axis due to a boost in longitudinal momentum caused by the color electric field. A measure of this separation should be a difference in the pseudorapidity ($\Delta\eta$) of the opposite sign pairs. This $\Delta\eta$ measure has a well define sign if we defined this difference measuring from the π^- to the π^+ . In order to form a correlation we must pick two pairs for comparison. The pairs have to come from the same tube (a final state of an expanded flux tube) since pairs originating from different tubes will not show this correlation. Therefore we require the π^+ and the π^- differ by 20° or less in ϕ . Let us call the first pair $\Delta\eta_1$. The next pair $\Delta\eta_2$ (having the same ϕ requirement) has to also lie inside the same tube to show this correlation. Thus we require that there is only 10° between the average ϕ of each pair. This implies that at most in ϕ no two pions can differ by more than 30° . In Figure 15 we show two pairs which would fall into the above cuts. $\Delta\eta_1$ and $\Delta\eta_2$ are positive in Figure 15 but if we would interchange the π^+ and π^- on either pair the value of its $\Delta\eta$ would change sign. Finally the mean value shown on Figure 15 is the mid-point between the π^+ and the π^- where one really uses the vector sum of the π^+ and the π^- which moves this point toward the harder pion.

Considering the above cuts we defined a correlation function where we combine pairs each having a $\Delta\eta$. Our variable is related to the sum of the absolute values of the individual $\Delta\eta$'s ($|\Delta\eta_1| + |\Delta\eta_2|$). We assign a sign to this sum such that if the sign of the individual $\Delta\eta$'s are the same it is a plus sign, while if they are different it is a minus sign. For the flux tube the color electric field extends over a large pseudorapidity range therefore let us consider the separation of pairs $|\Delta\eta|$ greater than 0.9. For the numerator of the correlation function we consider all combination of unique pairs ($\text{sign}(|\Delta\eta_1| + |\Delta\eta_2|)$) from a given central Au + Au event divided by a mixed event denominator created from pairs in different events. We determine the rescale of the mixed event denominator by considering the number of pairs of pairs for the case $|\Delta\phi|$ lying between 50° and 60° for events and mixed events so that the overall ratio of this sample numerator to denominator is 1. By picking $50^\circ < |\Delta\phi| < 60^\circ$ we make sure we are not choosing pairs from the same tube. For a simpler notation let ($\text{sign}(|\Delta\eta_1| + |\Delta\eta_2|)$) = $\Delta\eta_1 + \Delta\eta_2$ which varies from -4 to +4 since we have an overall η acceptance -1 to +1 (for the STAR TPC detector for which we calculated). The value being near ± 4 can happen when one has a hard pion with p_t of 4 GeV/c (upper cut) at $\eta = 1$ with a soft pion p_t of 0.8 GeV/c (lower cut) at $\eta = -1$ combined with another pair; a hard pion with p_t of 4 GeV/c at $\eta = -1$ with a soft pion with p_t of 0.8 GeV/c at $\eta = 1$.

In Figure 16 we show the correlation function of opposite sign charge-particle-pairs paired and binned by the variable $\Delta\eta_1 + \Delta\eta_2$ with a cut $|\Delta\eta|$ greater than 0.9 between the vector sums of the two pairs. The events are generated by the PBM[8] and are charged particles of $0.8 < p_t < 4.0$ GeV/c, and $|\eta| < 1$, from Au + Au central (0-10%) collisions at $\sqrt{s_{NN}} = 200$ GeV. Since we select pairs of pairs which are near each other in ϕ they all together pick up the tube correlation and thus these pairs of pairs overall show about a 4% correlation. In the $1.0 < \Delta\eta_1 + \Delta\eta_2 < 2.0$ region the correlation is 0.5% larger than the $-2.0 < \Delta\eta_1 + \Delta\eta_2 < -1.0$ region. This means there are more pairs of pairs aligned in the same direction compared to pairs of pairs not aligned. This alignment is what is predicted by the color electric field effect presented above. In fact if one has plus minus pairs all aligned in the same direction and spread across a pseudorapidity range, locally at any place in the pseudorapidity range one would observe an increase of unlike sign charge pairs compared to like sign charge pairs. At small $\Delta\eta$ unlike sign charge pairs are much larger than like sign charge pairs in both the PBM and the data which agree. See Figures. 10, 11, and 14 of Ref.[8]. Figure 11 compares the total correlation for unlike-sign charge pairs and like-sign charge pairs in the precision STAR central production experiment for Au + Au central (0-10%) collisions at $\sqrt{s_{NN}}=200$ GeV, in the transverse momentum range $0.8 < p_t < 2.0$ GeV/c[12]. The unlike-sign charge pairs are clearly larger in the region near $\Delta\phi = \Delta\eta = 0.0$. The increased correlation of the unlike-sign pairs is $0.8\% \pm 0.002\%$. Figure 10 shows that the PBM fit to these data gives the same results. Figure 14 shows that the CD = unlike-sign charge pairs minus like-sign charge pairs is positive for the experimental analysis. Therefore the unlike-sign charge pairs are considerably larger than the like-sign charge pairs. In fact this effect is so large and the alignment is so great that when one adds the unlike and like sign charge pairs correlations together there is still a dip at small $\Delta\eta$ and $\Delta\phi$ see Figure 4 and Figure 5 of this paper. The statistical significance of this dip in the two high precision experiments done independently from different data sets gathered 2 years apart[12, 14] is huge. It would require a fluctuation of 14σ to remove the dip. This dip is also not due to any systematic error since both of the just cited precision experiments carefully investigated that possibility; and found no evidence to challenge the reality of this dip. This highly significant dip ($\sim 14\sigma$) means that like-sign pairs are removed as one approaches the region $\Delta\eta = \Delta\phi = 0.0$. Thus this is very strong evidence for the predicted effect of the color electric field.

Let us now apply the above analysis to 0-10% central Au + Au collisions at $\sqrt{s_{NN}} = 200$ GeV. In figure 17 we show that aligned pairs positive $\Delta\eta_1 + \Delta\eta_2$ is 0.2% greater than not aligned pairs negative $\Delta\eta_1 + \Delta\eta_2$. This effect is about half the value we had simulated, but shows that this alignment effect is present in the data. We can obtain a measure of how significant this difference is by forming a ratio of not aligned(unlike) over aligned(like)(see Figure 18). If there was no effect the ratio would be a straight line at 1.0. We see that there is a dip of 0.2% at a $\Delta\eta_1 + \Delta\eta_2 = 1.4$ with an average value shift of 0.14% over the expected range.

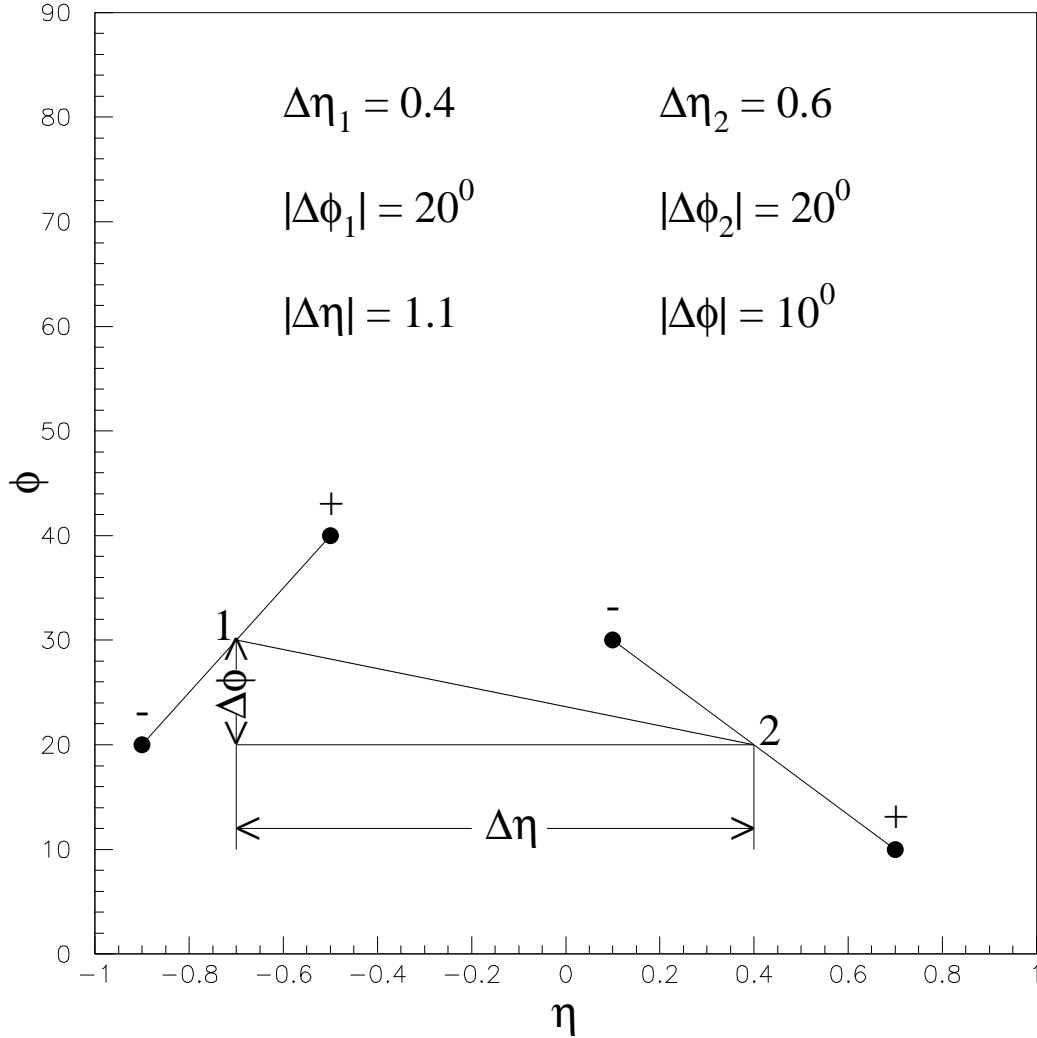


Figure 15: Pairs of pairs selected for forming a correlation due to the boost in longitudinal momentum caused by the color electric field. The largest separation we allow in ϕ for plus minus pair 1 is $\Delta\phi_1 = 20^0$. This assures the pair is in the same tube. The same is true for pair 2 so that it will also be contained in this same tube. The mid-point for pair 1 and 2 represents the vector sum of pair 1 and 2 which moves toward the harder particle when the momenta differ. These mid-points cannot be separated by more than 10^0 in $\Delta\phi$ in order to keep all four particles inside the same tube since the correlation function is entirely generated within the same tube. The $\Delta\eta$ measure is the angle between the vector sum 1 compared to the vector sum 2 along the beam axis (for this case $|\Delta\eta| = 1.1$). The positive sign for $\Delta\eta_1$ comes from the fact that one moves in a positive η direction from negative to positive. The same is true for $\Delta\eta_2$. If we would interchange the charge of the particles of the pairs the sign would change.

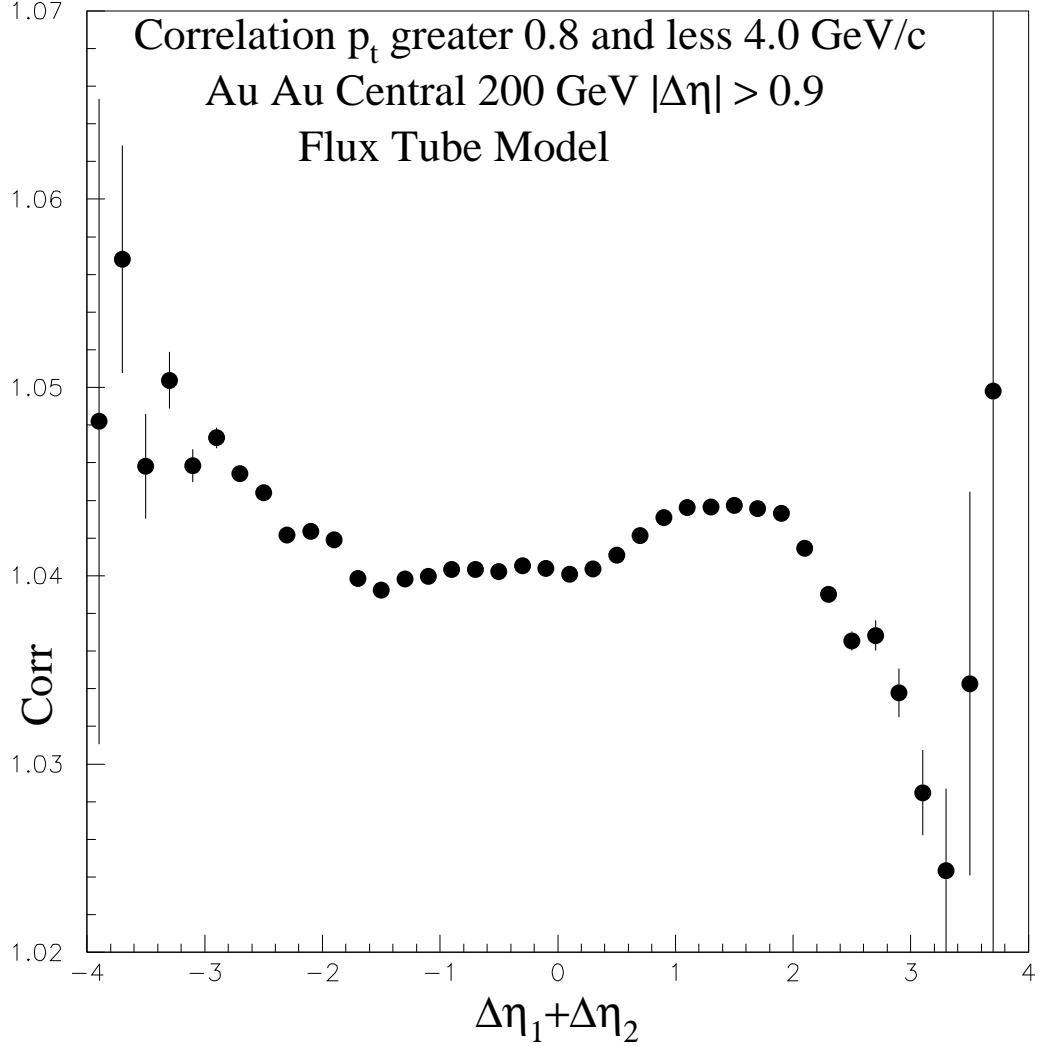


Figure 16: Correlation function of pairs formed to exhibit the effects of longitudinal momentum boosts by the color electric field as defined in the text. This correlation shows that there are more aligned pairs (correlation is larger by $\sim 0.5\%$ between $1.0 < \Delta\eta_1 + \Delta\eta_2 < 2.0$ compared to between $-2.0 < \Delta\eta_1 + \Delta\eta_2 < -1.0$). $\Delta\eta_1 + \Delta\eta_2$ is equal to $|\Delta\eta_1| + |\Delta\eta_2|$. As explained in the text this means there are more pairs of pairs aligned in the same direction compared to pairs not aligned as predicted by the color electric field. The signs and more detail are also explained in the text.

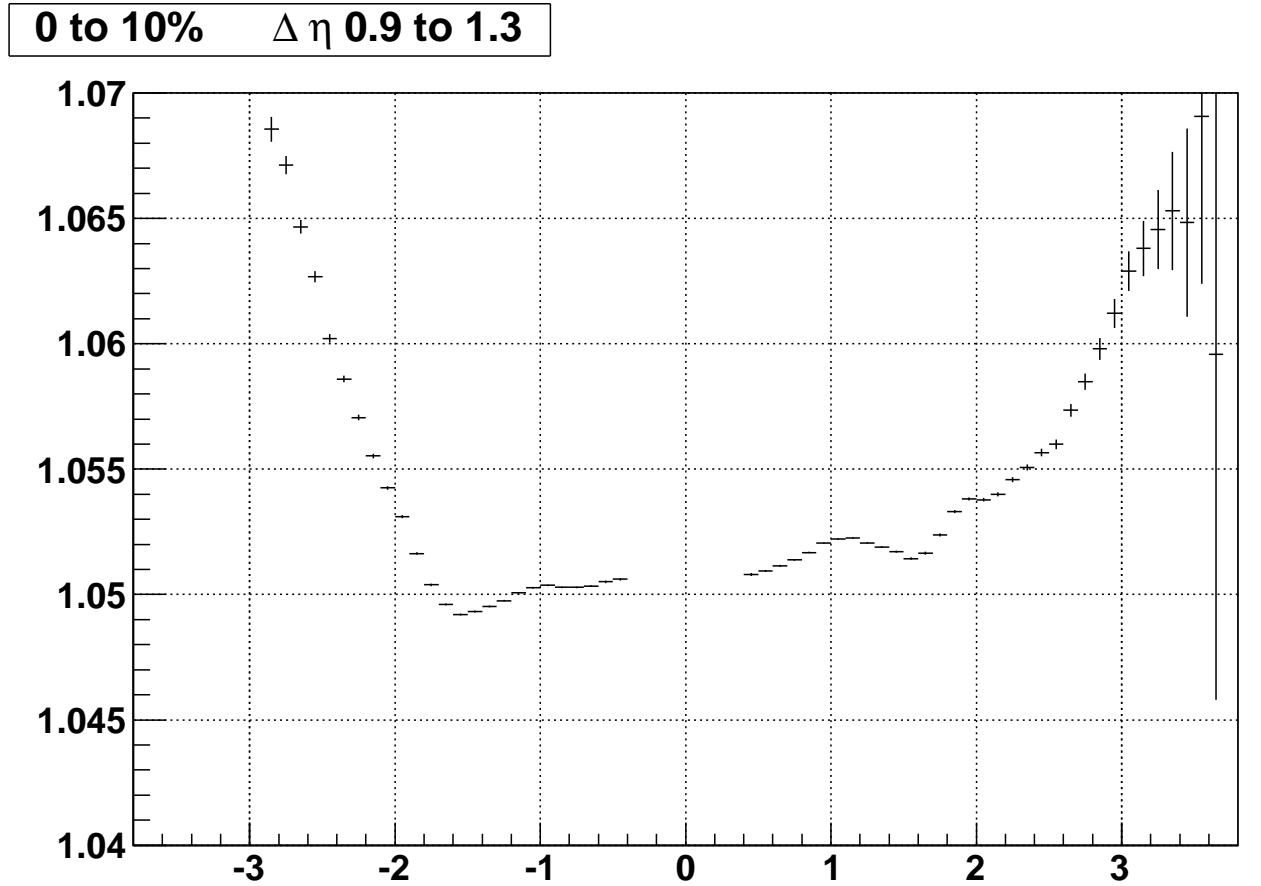


Figure 17: Correlation function of pairs formed to exhibit the effects of longitudinal momentum boosts by the color electric field as defined in the text. For this correlation we are using real 0-10% central Au + Au collisions at $\sqrt{s_{NN}} = 200$ GeV data. The aligned pairs positive values are larger by $\sim 0.2\%$ between $1.0 < \Delta\eta_1 + \Delta\eta_2 < 2.0$ than between $-2.0 < \Delta\eta_1 + \Delta\eta_2 < -1.0$). This means there are more pairs of pairs aligned in the same direction compared to pairs not aligned as predicted by the color electric field.

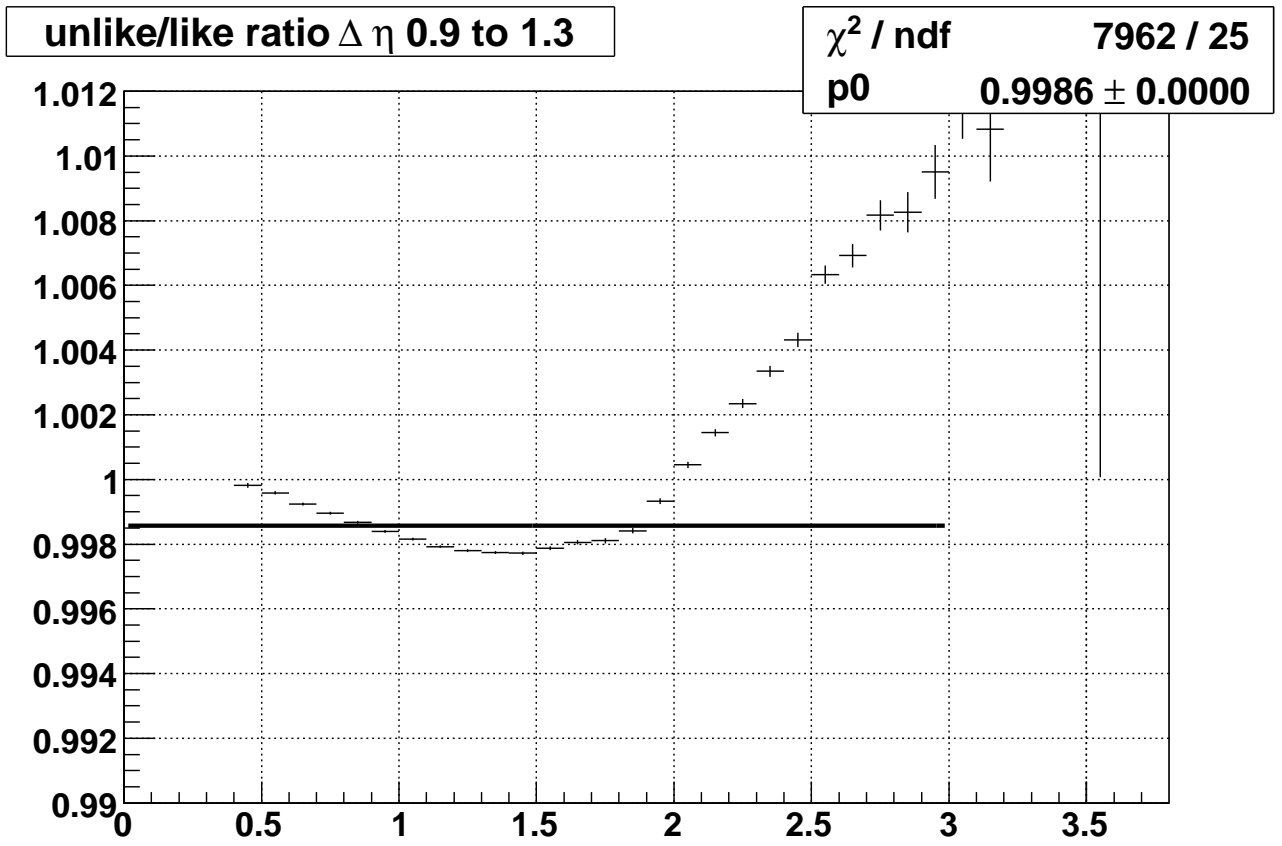


Figure 18: We can obtain a measure of how significant this difference is by forming a ratio of not aligned(unlike) over aligned(like). If there was no effect the ratio would be a straight line at 1.0. We see that there is a dip of 0.2% at a $\Delta\eta_1 + \Delta\eta_2 = 1.4$ with an average value shift of 0.14% over the expected range.

8 Color magnetic pionic measure and data.

After considering the color electric effect we turn to the color magnetic effect which causes up quarks to rotate around the flux tube axis in one direction, while the anti-up quarks rotate in the other direction. So when a pair of quarks and anti-quarks are formed they will pick up or lose transverse momentum. These changes in p_t will be transmitted to the π^+ and π^- pairs. In order to observe these differential p_t changes one must select pairs on one side of the tube in ϕ and compare to other pairs on the other side of the same tube which would lie around 40° to 48° away in ϕ . We defined a pair as a plus particle and minus particle with an opening angle (θ) of 16° or less. We are also interested in pairs that are directly on the other side of the tube. We require they are near in pseudorapidity ($\Delta\eta < 0.2$). The above requirements constrain the four charged particles comprising both pairs to be contained in the same tube and be close to being directly on opposite sides of the tube (a final state expanded flux tube). The difference in p_t changes due to and predicted by the color magnetic effect should give the π^+ on one side of the tube an increased p_t and a decreased p_t on the other side, while for the π^- it will be the other way around. This will lead to an anti-alignment between pairs. In Figure 19 we show two pairs which would fall into the above cuts. Both pairs are at the limit of the opening angle cut θ_1 and θ_2 equal 16° . The p_t of the plus particle for pair number 1 is 1.14 GeV/c, while the minus particle is 1.39 GeV/c. Thus ΔP_{t1} is equal to -0.25 GeV/c. The p_t of the plus particle for pair number 2 is 1.31 GeV/c, the minus particle is 0.91 GeV/c and ΔP_{t2} is equal to 0.40 GeV/c. Finally the mean value shown on Figure 19 is the mid-point between the π^+ and the π^- where one really uses the vector sum of the π^+ and the π^- which moves this point toward the harder pion.

Considering the above cuts we defined a correlation function where we combine pairs each having a ΔP_t . Our variable is related to the sum of the absolute values of the individual ΔP_t 's ($|\Delta P_{t1}| + |\Delta P_{t2}|$). We assign a sign to this sum such that if the sign of the individual ΔP_t 's are the same it is a plus sign, while if they are different it is a minus sign. For the flux tube the color magnetic field extends over a large pseudorapidity range where quarks and anti-quarks rotate around the flux tube axis, therefore we want to sample pairs at the different sides of the tube making a separation in ϕ ($\Delta\phi$) between 40° to 48° . We are interested in sampling the pairs on the other side so we require the separation in η ($\Delta\eta$) be 0.2 or less. For the numerator of the correlation function we consider all combination of unique pairs ($\text{sign}(|\Delta P_{t1}| + |\Delta P_{t2}|)$) from a given central Au + Au event divided by a mixed event denominator created from pairs in different events. We determine the rescale of the mixed event denominator by considering the number of pairs of pairs for the case $|\Delta\eta|$ lying between 1.2 and 1.5 plus any value of $|\Delta\phi|$ for events and mixed events so that the overall ratio of this sample numerator to denominator is 1. By picking this $\Delta\eta$ bin for all $|\Delta\phi|$ we have around the same pair count as the signal cut with the $\Delta\phi$ correlation of the tubes being washed out. For a simpler notation let $(\text{sign}(|\Delta P_{t1}| + |\Delta P_{t2}|)) = \Delta P_{t1} + \Delta P_{t2}$ which we plot in the range from -4 to +4 since we have an overall p_t range 0.8 to 4.0 GeV/c. Thus the maximum magnitude of ΔP_t 's is 3.2 GeV/c which makes $\Delta P_{t1} + \Delta P_{t2}$ have a range of ± 6.4 . However the larger values near these range limits occur very rarely.

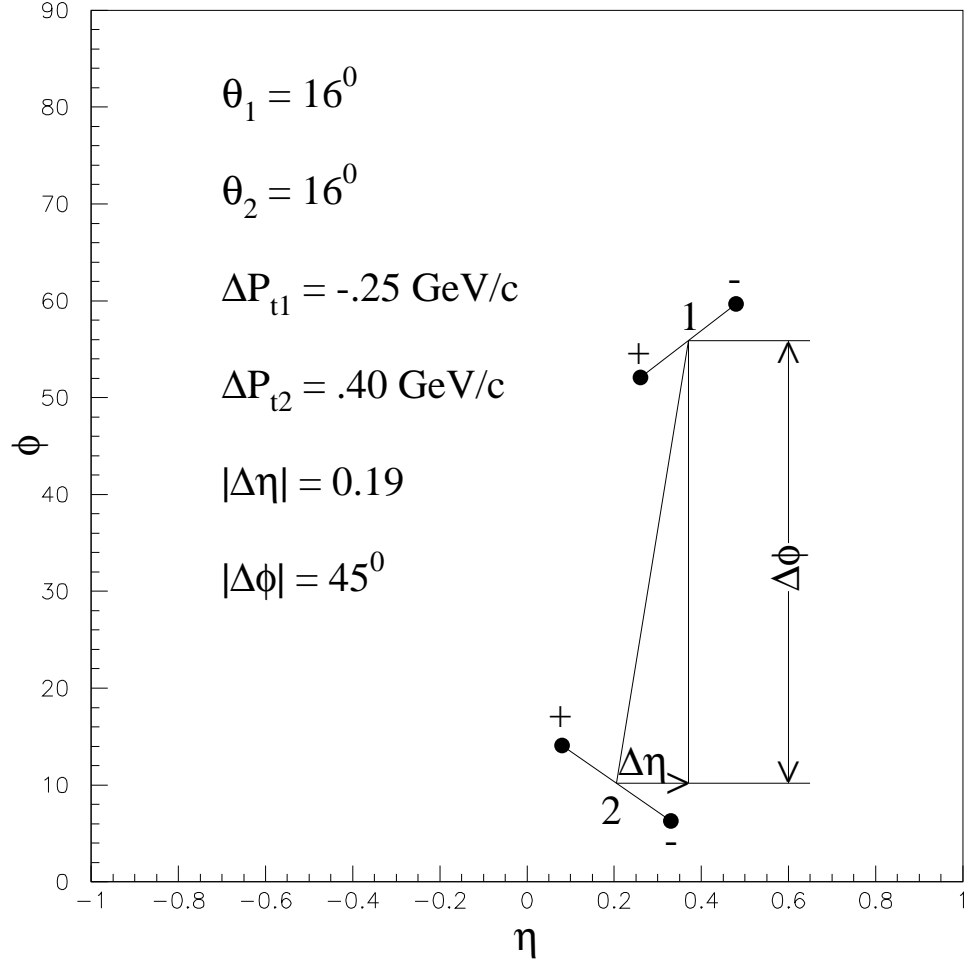


Figure 19: Pairs of pairs selected for forming a correlation exhibiting the effect of changes in p_t due to the color magnetic field. The largest opening angle θ for plus minus pairs is 16° or less. This opening angle assures that each pair has a high probability that it arises from a quark anti-quark pair. In this figure we have picked two pairs at this limit ($\theta_1 = 16^\circ$ and $\theta_2 = 16^\circ$). The mid-point for pair 1 and 2 represents the vector sum of pair 1 and 2 which moves toward the harder particle when the momenta differ. These mid-points are chosen to have $40^\circ < |\Delta\phi| < 48^\circ$ in order for the pairs to be on opposite sides of the tube. Since we are interested in pairs directly across the tube we make the $\Delta\eta$ separation be no more than 0.2. The difference in p_t for pair 1 is $\Delta P_{t1} = -0.25$ GeV/c, while the difference in p_t for pair 2 is $\Delta P_{t2} = 0.40$ GeV/c. The minus sign for 1 follows from the fact that the plus particle has 1.14 GeV/c and the minus particle has 1.39 GeV/c. The plus sign for 2 follows from the fact that the plus particle has 1.31 GeV/c and the minus particle has 0.91 GeV/c.

In Figure 20 we show the correlation function of opposite sign charged-particle-pairs paired and binned by the variable $\Delta P_{t1} + \Delta P_{t2}$ with a cut $|\Delta\eta|$ less than 0.2 between the vector sums of the two pairs, and with $40^\circ < |\Delta\phi| < 48^\circ$. The events are generated by the PBM[8] and are charged particles of $0.8 < p_t < 4.0$ GeV/c, with $|\eta| < 1$, from Au + Au central (0-10%) collisions at $\sqrt{s_{NN}} = 200$ GeV. Since we select pairs of pairs which are near each other in ϕ (40° to 48°) they all together pick up the tube correlation and thus these pairs of pairs overall show about a 0.4% correlation. In the $-4.0 < \Delta P_{t1} + \Delta P_{t2} < -1.0$ region the correlation increases from 0.4% to 1%, while in the $1.0 < \Delta P_{t1} + \Delta P_{t2} < 4.0$ region the correlation decreases from 0.4% to -0.2%. This means the pairs of pairs are anti-aligned at a higher rate than aligned. This anti-alignment is what is predicted by the color magnetic field effect presented above. In fact the anti-alignment increases with p_t as the ratio tube particle to background increases.

We apply the magnetic analysis to 0-10% central Au + Au collisions at $\sqrt{s_{NN}} = 200$ GeV. The error bars on the correlation is such that we need increase our $\Delta\phi$ cut to $32^\circ < |\Delta\phi| < 48^\circ$. The STAR TPC efficiency varied with azimuthal angle because of sector boundaries in the TPC. 12 boundaries generate effects every 30° . Pairs of pairs have a lower efficiency if separated by 30° . Pairs that lie with a ϕ separation between 25° and 35° have both pairs going into sector boundaries in twelve orientations in the TPC. This efficiency is less than other angles where one of its pairs will go into sector boundaries at 24 orientations in the TPC. Thus the numerator of the correlation is reduced more in the TPC data. In figure 21 we show that aligned pairs positive $\Delta P_{t1} + \Delta P_{t2}$ is 0.1% less than not aligned pairs negative $\Delta P_{t1} + \Delta P_{t2}$. This is about half the value that we had simulated, and shows that this alignment effect is present in the data. The average value of the correlation has been reduced because of the TPC efficiency. We can obtain a measure of how significant this difference is by forming a ratio of not aligned(unlike) over aligned(like)(see Figure 22). If there was no effect the ratio would be a straight line at 1.0. We see that there is a rise of 0.1% in a parabolic shape which is a good fit at a $\Delta P_{t1} + \Delta P_{t2} = 2.0$.

9 Summary and Discussion

In this paper we discuss a Glasma Flux Tube Model(GFTM)[1] which has tubes of parallel strong color QCD electric and magnetic fields that are generated by the initial conditions of Au + Au central collisions at $\sqrt{s_{NN}}=200$ GeV. We summarize the assumptions made and the reasoning that led to the development and construction of GFTM, which successfully explained the charge-particle-pair correlations in the central (0-10% centrality) $\sqrt{s_{NN}} = 200$ GeV Au Au data[12].

In the GFTM a flux tube is formed right after the initial collision of the Au Au system. This flux tube extends over many units of pseudorapidity ($\Delta\eta$). A blast wave gives the tubes near the surface transverse flow. Initially the transverse space is filled with flux tubes of large longitudinal extent but small transverse size $\sim Q_s^{-1}$. The flux tubes that are near the surface of the fireball get the largest radial flow and are emitted from the surface. These partons shower and the higher p_t particles escape the surface and do not interact. Q_s is around 1

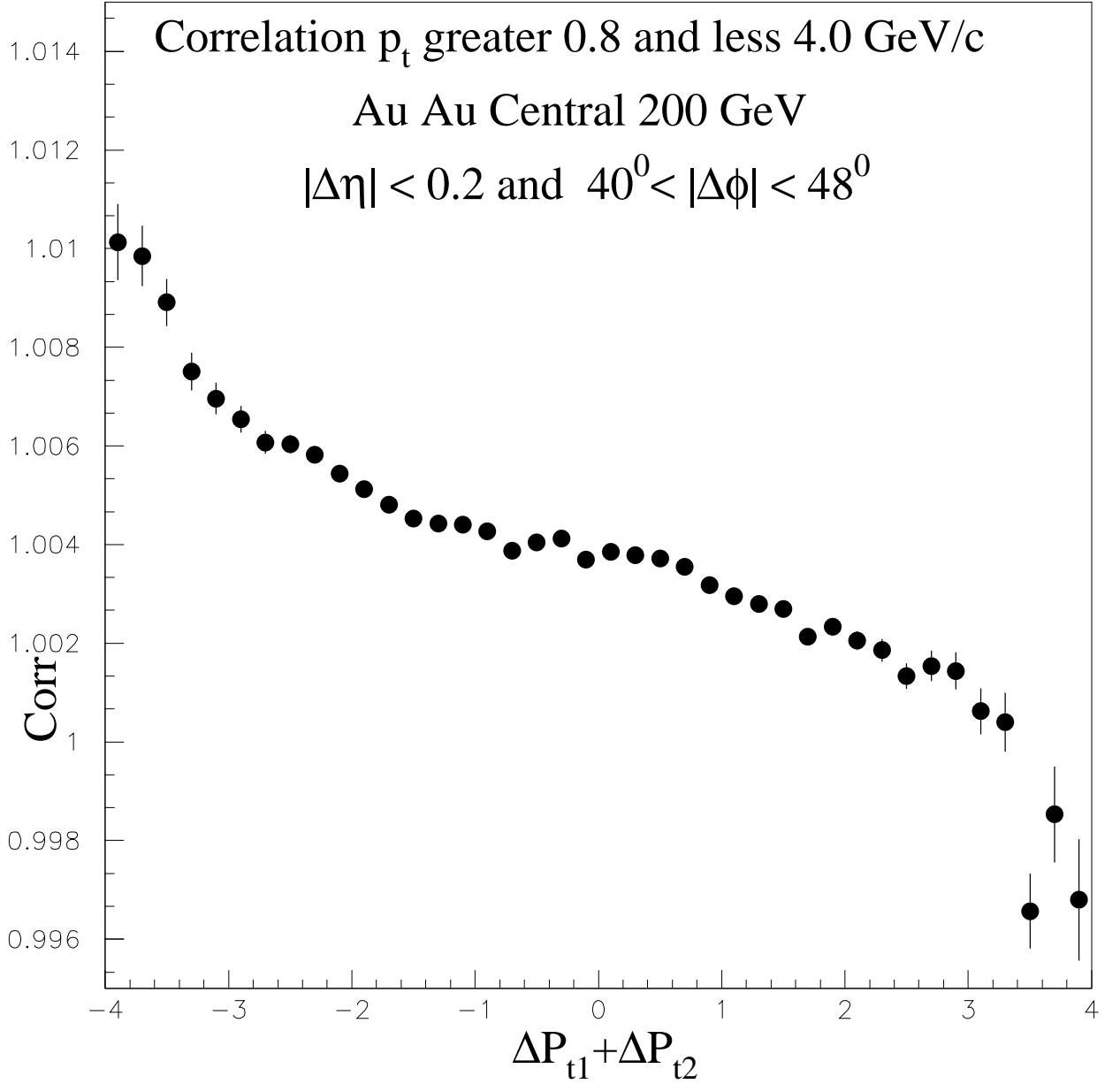


Figure 20: Correlation function of pairs of pairs formed for exhibiting the effect of changes in p_t due to the color magnetic field as defined in the text. This correlation shows that there are more anti-aligned pairs. The correlation is larger by $\sim 1.2\%$ for $\Delta P_{t1} + \Delta P_{t2} = -4.0$ compared to $\Delta P_{t1} + \Delta P_{t2} = 4.0$. $\Delta P_{t1} + \Delta P_{t2}$ is equal to $|\Delta P_{t1}| + |\Delta P_{t2}|$ where the sign is also explained in the text.

0 to 10% $\Delta\phi$ 32 to 48

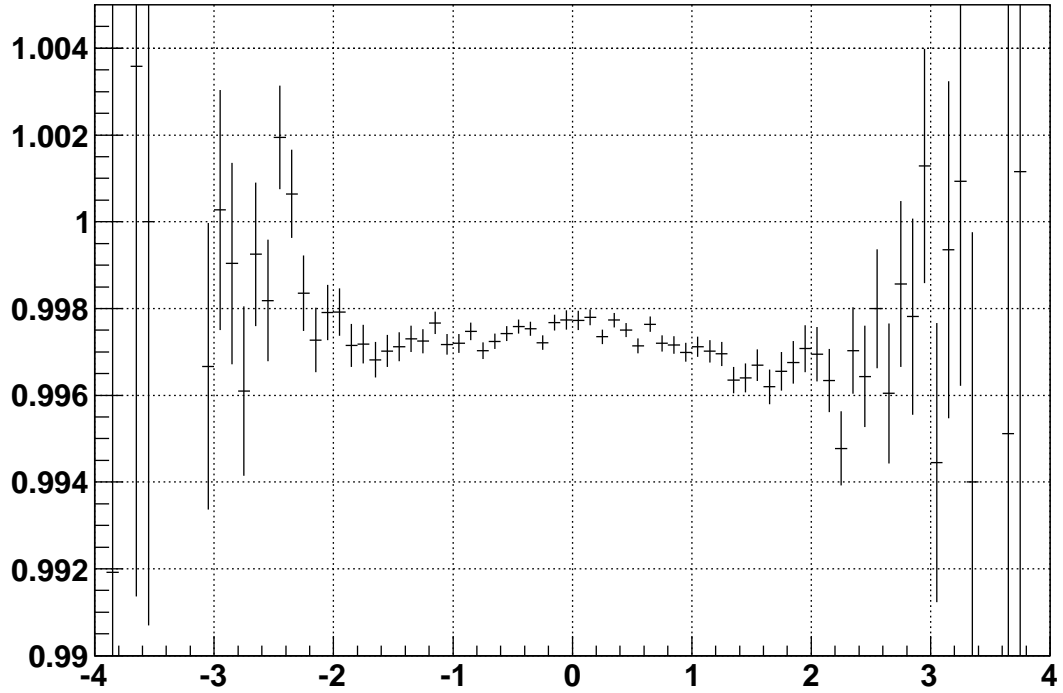


Figure 21: Correlation function of pairs of pairs formed for exhibiting the effect of changes in p_t due to the color magnetic field as defined in the text. This correlation shows that there are more anti-aligned For this correlation we are using real 0-10% central Au + Au collisions at $\sqrt{s_{NN}} = 200$ GeV data. The not aligned pairs negative values are larger by $\sim 0.1\%$ at $-2.0 \Delta P_{t1} + \Delta P_{t2}$. This means there are more pairs of pairs aligned in the opposite direction compared to pairs aligned as predicted by the color magnetic field.

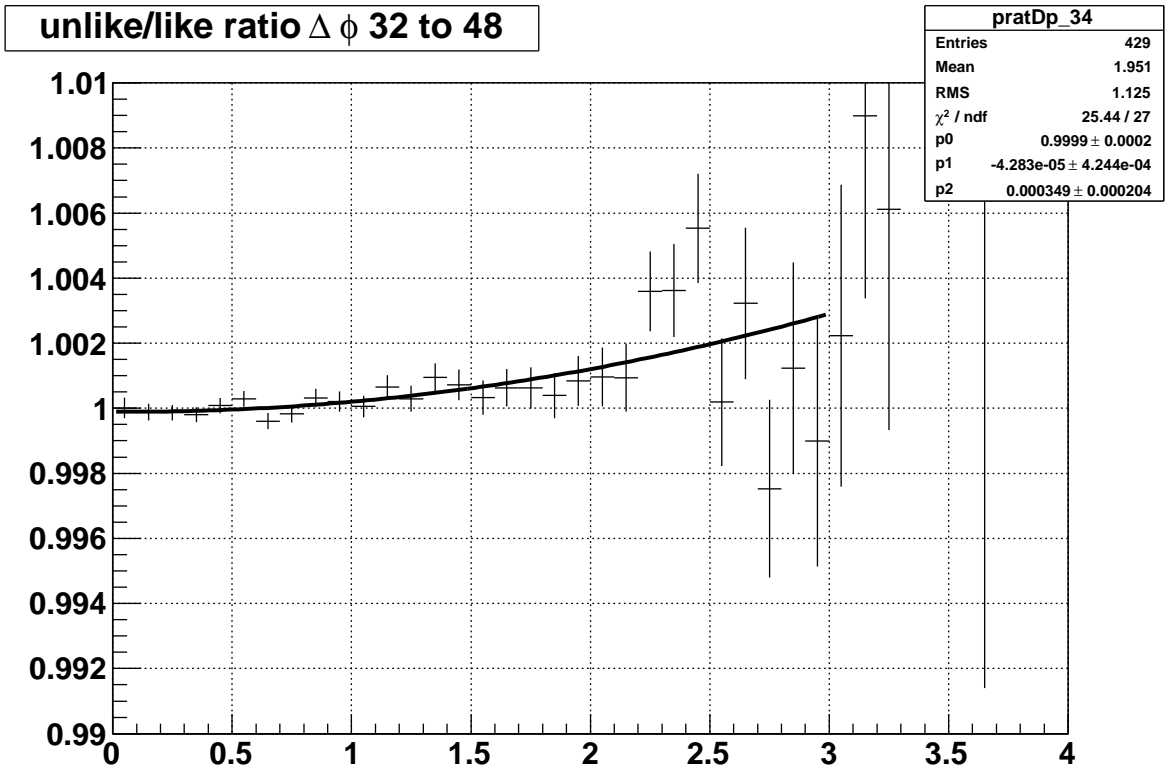


Figure 22: We can obtain a measure of how significant this difference is by forming a ratio of not aligned(unlike) over aligned(like). If there was no effect the ratio would be a straight line at 1.0. We see that there is a rise of 0.1% in a parabolic shape which is a good fit at a $\Delta P_{t1} + \Delta P_{t2} = 2.0$.

GeV/c thus the size of the flux tube is about 1/4 fm initially. The flux tubes near the surface are initially at a radius ~ 5 fm. The ϕ angle wedge of the flux tube $\sim 1/20$ radians or $\sim 3^\circ$. The flux tubes on the surface turn out to be on the average 12 in number. They form an approximate ring about the center of the collision see Figure 1. The twelve tube ring creates the average behavior of tube survival near the surface of the expanding fire ball of the blast wave. The final state surface tubes that emit the final state particles at kinetic freezeout for this paper are given by the PBM[8]. One should note that the blast wave surface is moving at its maximum velocity at freezeout ($3c/4$).

We explored the charge dependence correlation where we separate pairs into like sign pairs and unlike sign pairs. In Figure 11 we show the unlike sign pair correlation of the single flux tube and the background subtracted data. In Figure 12 we show the same for like sign pairs. We see in both Figure 11 and Figure 12, that the correlation from each pair choice is well described by GFTM. We see at small $\Delta\phi, \Delta\eta$ there is a local bump for unlike sign pairs, while there is negative bump or dip for like sign pairs. This dip or hole torn is caused by QCD field shown in Figure 13. This field focus unlike charge pairs into the same $\Delta\phi, \Delta\eta$ and defocus like charge pairs out of this same region.

Strong CP violation (Chern-Simons topological charge) is treated in Sec. 6.

We develop a predictive pionic measure of the strong CP Violation. The GFTM flux tubes are made up of longitudinal color electric and magnetic fields which generate topological Chern-Simons charge[5] through the $F\tilde{F}$ term that becomes a source of CP violation. The color electric field which points along the flux tube axis causes an up quark to be accelerated in one direction along the beam axis, while the anti-up quark is accelerated in the other direction. So when a pair of quarks and anti-quarks are formed they separate along the beam axis leading to a separated π^+ and π^- pair along this axis. The color magnetic field which also points along the flux tube axis (which is parallel to the beam axis) causes an up quark to rotate around the flux tube axis in one direction, while the anti-up quark rotates in the other direction. So when a pair of quarks and anti-quarks are formed they will pick up or lose transverse momentum. These changes in p_t will be transmitted to the π^+ and π^- pairs.

The above pionic measures of strong CP violation are used to form correlation functions based on four particles composed of two pairs which are opposite sign charge-particle-pairs that are paired and binned. These four particle correlations accumulate from tube to tube by particles that are pushed or pulled (by the color electric field) and rotated (by the color magnetic field) in a right or left handed direction. The longitudinal color electric field predicts aligned pairs in a pseudorapidity or $\Delta\eta$ measure. The longitudinal color magnetic field predicts anti-aligned pairs in a transverse momentum or ΔP_t measure. We observe in the STAR TPC $\sqrt{s_{NN}} = 200$ GeV central Au Au collision data that these correlations are as expected and is a strong confirmation of this theory(see Sec. 7 and Sec. 8). The much larger unlike-sign pairs than like-sign pairs in the data and the strong dip of the CI correlation at small $\Delta\eta$ (see Sec. 5) shows very strong evidence supporting the color electric alignment prediction in the $\sqrt{s_{NN}} = 200$ GeV central Au Au collision data analyses at RHIC[8, 12]. This highly significant dip ($\sim 14\sigma$) means that like-sign pairs are removed as one approaches the region $\Delta\eta = \Delta\phi = 0.0$. Thus this is the strongest evidence for the predicted effect of

the color electric field.

10 Acknowledgments

This research was supported by the U.S. Department of Energy under Contract No. DE-AC02-98CH10886. The author thanks Sam Lindenbaum and William Love for valuable discussion and Bill for assistance in production of figures. It is sad that both are now gone.

References

- [1] A. Dumitru, F. Gelis, L. McLerran and R. Venugopalan, Nucl. Phys. A 810 (2008) 91.
- [2] L. McLerran and R. Venugopalan, Phys. Rev. D 49 (1994) 2233; Phys. Rev. D 49 (1994) 3352; Phys. Rev. D 50 (1994) 2225.
- [3] T. Lappi and L. McLerran, Nucl. Phys. A 772 (2006) 200.
- [4] F. Gelis and R. Venugopalan, Acta Phys. Polon. B 37 (2006) 3253.
- [5] D. Kharzeev, A. Krasnitz and R. Venugopalan, Phys. Lett. B 545 (2002) 298.
- [6] P. Romatschke and R. Venugopalan, Phys. Rev. D 74 (2006) 045011.
- [7] S. Gavin, L. McLerran and G. Moschelli, Phys. Rev. C 79 (2009) 051902.
- [8] S.J. Lindenbaum, R.S. Longacre, Eur. Phys. J. C. 49 (2007) 767.
- [9] S.J. Lindenbaum, R.S. Longacre, arXiv:0809.2286[Nucl-th].
- [10] T. Sjostrand, M. van Zijil, Phys. Rev. D 36 (1987) 2019.
- [11] J. Adams *et al.*, Phys. Rev. C 71 (2005) 044906, S.S. Adler *et al.*, Phys. Rev. Lett. 93 (2004) 152302.
- [12] J. Adams *et al.*, Phys. Rev. C 75, 034901 (2007).
- [13] S.J. Lindenbaum and R.S. Longacre, Phys. Rev. C 78 (2008) 054904.
- [14] B.I. Abelev *et al.*, arXiv:0806.0513[nucl-ex].
- [15] B. Alver and G. Roland, Phys. Rev. C 81 (2010) 054905.
- [16] C. Vafa, E. Witten, Phys. Rev. Lett. 53 (1984) 535, Nucl. Phys. B 234 (1984) 173.
- [17] D. Kharzeev, R.D. Pisarski, M.H.G. Tytgat, Phys. Rev. Lett. 81 (1998) 512.
- [18] D. Kharzeev, R.D. Pisarski, Phys. Rev. D 61 (2000) 111901.